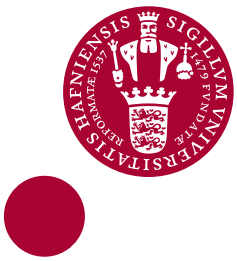

Pelagic microbial heterotrophy in response to a highly productive bloom of Phaeocystis antarctica in the Amundsen Sea Polynya, Antarctica

Williams, C. M.; Dupont, A.m.; Loevenich, J.; Post, A. F.; Dinasquet, Julie Vanessa; Yager, P. L.

Published in:
Elementa : Science of the Anthropocene

DOI:
10.12952/journal.elementa.000102

Publication date:
2016

Document version
Publisher's PDF, also known as Version of record

ELEMENTA
Science of the Anthropocene

Pelagic microbial heterotrophy in response to a highly productive bloom of *Phaeocystis antarctica* in the Amundsen Sea Polynya, Antarctica

C.M. Williams[1] • A.M. Dupont[1] • J. Loevenich[1] • A.F. Post[2] • J. Dinasquet[3,4] • P.L. Yager [1*]

[1]Department of Marine Sciences, The University of Georgia, Athens, Georgia, United States
[2]Graduate School of Oceanography, URI, Narragansett, Rhode Island, United States
[3]Marine Biological Section, University of Copenhagen, Helsingør, Denmark
[4]Department of Natural Sciences, Linnaeus University, Kalmar, Sweden

*pyager@uga.edu

Abstract

Heterotrophic bacteria play a key role in marine carbon cycling, and understanding their activities in polar systems is important for considering climate change impacts there. One goal of the ASPIRE project was to examine the relationship between the phytoplankton bloom and bacterial heterotrophy in the Amundsen Sea Polynya (ASP). Bacterial abundance, production (BP), respiration, growth efficiency, and extracellular enzyme activity (EEA) were compared to nutrient and organic matter inventories, chlorophyll *a* (Chl *a*), viral and microzooplankton abundance, and net primary production (NPP). Bacterial production and respiration clearly responded (0.04–4.0 and 10–53 μg C L^{-1} d^{-1}, respectively) to the buildup of a massive *Phaeocystis antarctica* bloom (Chl *a*: 0.2–22 μg L^{-1}), with highest rates observed in the central polynya where Chl *a* and particulate organic carbon (POC) were greatest. The highest BP rates exceeded those reported for the Ross Sea or any other Antarctic coastal system, yet the BP:NPP ratio (2.1–9.4%) was relatively low. Bacterial respiration was also high, and growth efficiency (2–27%; median = 10%) was similar to oligotrophic systems. Thus, the integrated bacterial carbon demand (0.8–2.8 g C m^{-2} d^{-1}) was a high fraction (25–128%; median = 43%) of NPP during bloom development. During peak bloom, activity was particle-associated: BP and EEA correlated well with POC, and size fractionation experiments showed that the larger size fraction (> 3 μm) accounted for a majority (~ 75%) of the BP. The community was psychrophilic, with a 5x reduction in BP when warmed to 20°C. In deeper waters, respiration remained relatively high, likely fueled by the significant downward particle flux in the region. A highly active, particle-associated, heterotrophic microbial community clearly responded to the extraordinary phytoplankton bloom in the ASP, likely limiting biological pump efficiency during the early season.

Domain Editor-in-Chief
Jody W. Deming, University of Washington

Knowledge Domain
Ocean Science

Article Type
Research Article

Part of an *Elementa* Special Feature
ASPIRE: The Amundsen Sea Polynya International Research Expedition

Received: December 1, 2015
Accepted: March 18, 2016
Published: April 21, 2016

Introduction

As air and ocean temperatures rise with global climate change, polar ecosystems are particularly vulnerable (Schofield et al., 2010) and changing rapidly (Stammerjohn et al., 2008, 2015). In the coastal Southern Ocean, where terrestrial inputs are negligible, phytoplankton are the primary source of organic matter to the marine system, and heterotrophy is directly tied to the annual primary production. Coastal polynyas are hot spots for both biological productivity (Smith and Barber, 2007) and air-sea exchange (Mu et al., 2014). Primary productivity in Antarctic coastal polynyas ranges up to 105 ± 22 g C m^{-2} yr^{-1} (Arrigo et al., 2015) while the open Southern Ocean (south of 50 °S) averages 57 g C m^{-2} yr^{-1} (Arrigo et al., 2008). In coastal areas, the

seasonal sea ice reduction induced by climate change is expected to enhance light penetration, which would increase primary production, but may also increase surface wind stress that would deepen the upper mixed layer (Ducklow et al., 2013) and reduce phytoplankton productivity (e.g., Montes-Hugo et al., 2009).

Primary production in Antarctic polynyas tends to be dominated by diatoms along the marginal ice zone, and by the haptophyte *Phaeocystis antarctica* in open waters (Arrigo et al., 1999; Alderkamp et al., 2012). Although *P. antarctica* has a unicellular life stage, in the photic zone of Antarctic waters it is most commonly found in dense colonial assemblages (Kennedy et al., 2012). Key questions relevant to the carbon cycle of polynyas include whether potentially high rates of net primary production (NPP) are matched by comparably high rates of heterotrophic activity, and what impact the microbial heterotrophs have on the export flux. In the Ross Sea Polynya, a high particulate concentration near the surface has been shown to yield large vertical fluxes of organic matter (Smith et al., 2011).

The Amundsen Sea hosts the most productive polynya (per unit area) in the Southern Ocean (Arrigo and van Dijken, 2003; Arrigo et al., 2015), yet it is one of the most remote and least studied. The Amundsen Sea Polynya (ASP) extends, on average, 27,333 ± 8749 km^2 (1997–2010 October–March mean open water; Arrigo et al., 2012), and up to 80,000 km^2 at its maximum extent in mid-January) and is only accessible by icebreaker for a few months during the austral summer (Yager et al., 2012). While iron (Fe) concentrations have been shown to limit phytoplankton growth throughout the Southern Ocean (Martin et al., 1990; Smith et al., 2013), the ASP receives substantial Fe inputs from ice-sheet-ocean interactions, which support the intense seasonal blooms observed there (Yager et al., 2012; Sherrell et al., 2015).

While there is some indication in the literature for rate limitation due to temperature, psychrophilic bacteria are primarily limited by dissolved organic matter (DOM) flux in cold waters (Pomeroy and Wiebe, 2001) and can clearly respond strongly to high-latitude phytoplankton blooms (Yager et al., 2001). Unlike in the Arctic, which receives a large DOM supply from rivers (Feng et al., 2013), Antarctic DOM supply is linked primarily to phytoplankton productivity, with secondary sources from ice sheet degradation and deep waters (Dubnick et al., 2010). DOM flux is also influenced by macro- and micro-zooplankton (Steinberg et al., 2004), which can be spotty and have low abundance in these regions (Dolan et al., 2013; Wilson et al., 2015). As part of the Amundsen Sea Polynya International Research Expedition (ASPIRE) project (December 2010–January 2011), our goal was to determine how the heterotrophic bacterial community responded to the dense, spring phytoplankton bloom. Here we report pelagic microbial biomass and activity in the context of an early season *Phaeocystis* bloom in the ASP and comment on the impact of the microbial community on the bloom's fate.

Methods

Sampling

ASPIRE examined the polynya region onboard the RVIB *Nathaniel B. Palmer* (NBP10-05) between 14 December 2010 and 8 January 2011 (Yager et al., 2012). Here, we report data from 13 stations within and around the edges of the ASP (Table 1; Figure 1) where a full suite of inventory and rate measurements was obtained from the upper water column. A few additional data are reported for comparison from samples collected during a previous visit to the region onboard the Swedish IB *Oden* (OSO 2007–2008 Station 16; Table 1; Figure 1).

Ice concentrations at the time of sampling were determined from unprojected AMSR-E 12.5-km satellite images (see Mu et al., 2014). Open water duration (OWD) was computed from the number of days (since August 1) that each station exhibited less than 50% ice cover including the day that we sampled it (Yager et al., 2016). Over the course of ASPIRE, the average open water area (< 50% ice cover as observed from 26 daily images) was 49,160 ± 9,952 km^2.

Hydrographic profiles and discrete water samples were collected from each station using a conventional shipboard conductivity-temperature-depth (CTD; Sea-Bird 911+) sensor and a 24 x 10 L Niskin bottle rosette sampler (General Oceanics). Potential temperature (θ) and salinity (S) were recorded continuously as a function of depth and at the time of Niskin bottle closure. Discrete water samples for microbial biomass and activity experiments were collected from 13 stations (Figure 1) at 5–7 depths in the upper 100 m, 1–3 depths below 100 m. Samples from *Oden* were collected similarly. Most samples (> 75%) were collected in the upper 400 m of the water column. Shelf water depths in this area range from 300 to 1600 m (Nitsche et al., 2007).

Inorganic nutrients, Chlorophyll a, organic matter, and primary production

Water samples for chemical and biological inventories and rates were collected at the same stations and depths as above and then processed for dissolved inorganic nitrogen (DIN = nitrate + nitrite + ammonium) and phosphorous (DIP), particulate and dissolved organic carbon and nitrogen (POC, PON, DOC, DON), chlorophyll *a* (Chl *a*), and primary production according to standard protocols (Knap et al., 1996). These data are more fully described elsewhere (see Yager et al., 2016). The ^{14}C-bicarbonate uptake rates for primary

Table 1. Station information, including ice conditions, and integrated (0–100 m depth) microbial inventories and rates

Station number[a]	Lat (°)	Long (°)	Seafloor depth (m)	Year day sampled	Sea ice conc.	Open water duration (d)	Surface mixed layer depth[b] (m)	ΔDIN_{100} (mmol N m^{-2})	Chl *a* (mg m^{-2})	Bacterial biomass (mmol C m^{-2})	Bacterial production (mmol C m^{-2} d^{-1})
OSO 2007–2008											
16	–73.94	–115.67	1248	352	0%	-	100	575	384	40	19
ASPIRE 2010–2011											
5	–73.97	–118.03	1250	348	26%	26	28	58	180	59	1.8
68	–71.86	–118.28	830	373	68%	8	14	160	70	-[c]	4.4
66	–72.74	–116.02	659	370	85%	14	10	370	300	67	11
13	–73.57	–112.67	550	352	0%	56	42	380	620	51	14
34	–72.96	–115.76	684	358	38%	12	11	440	680	53	12
25	–73.12	–112.00	406	356	0%	38	16	500	500	61	10
50	–73.42	–115.25	1050	363	0%	43	19	560	440	58	13
6	–73.18	–115.00	770	349	36%	15	10	560	550	36	11
35	–73.28	–112.10	420	361	0%	48	22	630	690	50	18
48	–73.70	–115.45	997	362	0%	46	22	630	830	81	16
18	–73.00	–113.30	435	355	5%	24	15	660	660	82	10
29	–73.35	–114.13	738	357	0%	41	32	700	760	36	13
57	–73.71	–113.27	745	365	0%	61	81	740	590	123	11
AVE[d]	-	-	733	359	20%	33	25	490	528	58	11
STD	-	-	256	8	29%	18	19	210	226	29	4.3
n	-	-	13	13	13	13	13	13	13	12	13
$R_{\Delta DIN}$[e]	–0.27	**0.70**	–0.41	0.01	**–0.59**	0.52	0.30	**1.0**	**0.82**	0.29	**0.74**

[a]OSO 2007–2008 refers to the Swedish *Oden Southern Ocean* expedition of that year; ASPIRE stations are arranged in order of increasing nitrogen drawdown (ΔDIN_{100}).
[b]As defined by ΔT method described by Alderkamp et al. (2015).
[c]Abundance data from Station 68 were considered erroneous (see text).
[d]Average values for the ASPIRE data sets.
[e]Correlation coefficient for the relationship between ΔDIN_{100} and the variables listed; bold indicates $p < 0.05$.
doi: 10.12952/journal.elementa.000102.t001

production are considered net primary production (NPP) since 24 h incubations gave bulk incorporation into particulate cellular material. For this paper, we used principal component analysis (PCA) to convert the set of often highly correlated physical and biogeochemical variables into a set of uncorrelated variables called principal components (PC), against which we compared our observations of microbial activity.

Microbial abundance and activity

Bacterial abundance samples were collected in triplicate from Niskin bottles at eight depths per station, preserved using 1% paraformaldehyde, and deep frozen (–80 °C) until they were processed at the University of Georgia. Flow cytometry was used to count bacterial cells with SYBR Green nucleic acid stain (Marie et al., 1997). Flow cytometer abundance was calibrated with polystyrene beads and values were cross-checked using DAPI and epifluorescence microscopy (Porter and Feig, 1980). Abundance was converted to bacterial carbon (BAC) using a conversion factor (25 fg C $cell^{-1}$; Simon and Azam, 1989). Precision was ± 3%.

Viral abundance at five depths per station was determined similarly using flow cytometry at the University of Copenhagen (Marie et al., 1999). Microzooplankton abundance was determined at three depths per station using microscopy (Goswami, 2004) or flow cytometry (Christaki et al., 2011; for details see Yager et al., 2016).

Bacterial production (BP) was measured in triplicate at eight depths per station using the microcentrifuge method for ^{3}H-leucine incorporation into protein (Kirchman et al., 1985; Smith and Azam, 1992; Ducklow, 2000; Kirchman, 2001). Samples were incubated for 4 h in the dark, at water bath temperatures set to within 0.5 °C of *in situ* temperature, with 25 nmol L^{-1} ^{3}H-leucine, and then compared to killed controls. Initial experiments confirmed that the standard 25 nmol L^{-1} addition was adequate for the desired saturation (see for example Simon and Azam, 1989; Ducklow et al., 2000, Buesing and Gessner, 2003) while achieving linear rates over 4 h (no induction). Following protein extraction, Ultima Gold scintillation cocktail was added and allowed to stand overnight. Incorporated radiation was determined using a Beckman LS 6500 liquid scintillation counter onboard for 5 min per sample. Activity measured in killed controls was subtracted from the sample values, eliminating any isotope adsorption to particulate protein. Activities were converted to incorporated leucine using specific activity and standard quench controls.

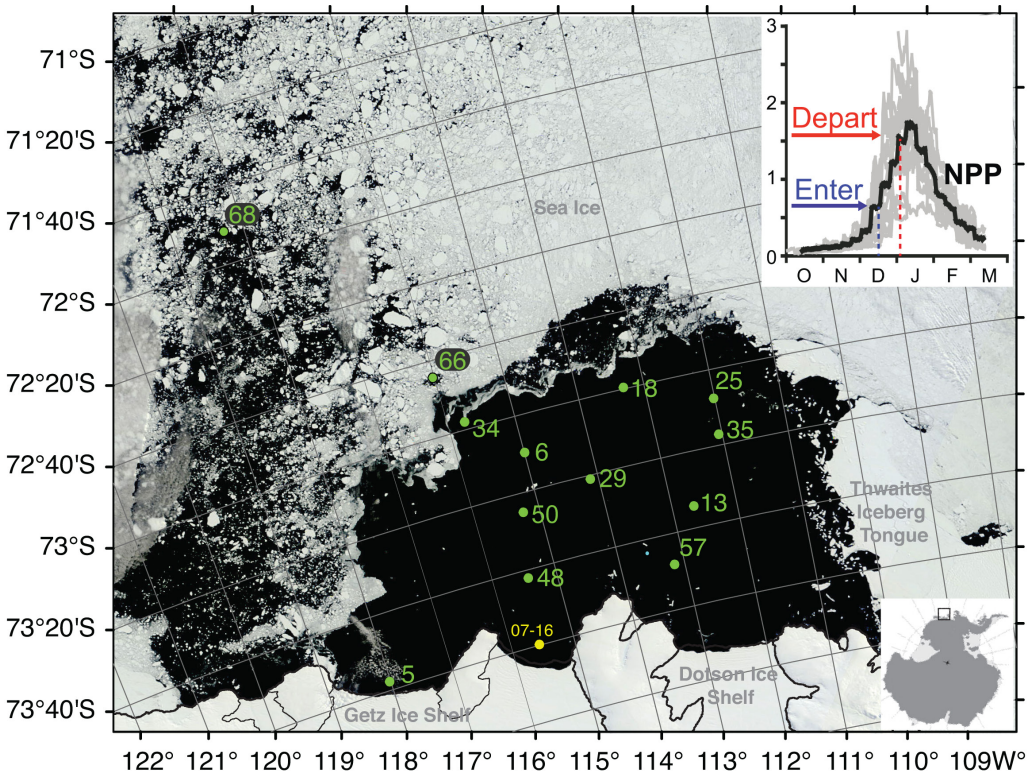

Figure 1
Map of study area.

A map of the study area projected onto a MODIS image (2 January 2011) of sea ice (mottled white), glacial ice (solid white), and open water (black). ASPIRE station numbers and locations are shown in green; OSO Station 16 (from the Swedish *Oden* expedition in 2007–2008) is shown in yellow. Lower right inset locates the region relative to the Antarctic continent. Upper right inset shows timing of ASPIRE sampling effort relative to the 1997–2014 climatology of daily net primary production (NPP; mg C m^{-2} d^{-1}; black) with interannual variability (gray) over the bloom season (October-March; modified from Arrigo et al., 2015).

doi: 10.12952/journal.elementa.000102.f001

Rates of incorporated leucine (pmol leu L^{-1} h^{-1}) were converted to BP (µg C L^{-1} d^{-1}) using a standard conversion factor (CF =1.5 kg C mol $leucine^{-1}$, based on 131.2 g-leucine $mol\text{-}leucine^{-1}$, 13.699 g-protein $g\text{-}leucine^{-1}$, and 0.86 g-C $g\text{-}protein^{-1}$; Simon and Azam, 1989; Kirchman, 2001; Ducklow et al., 1992, 2002) that is lower than or equal to that used for the Ross Sea (Ducklow, 2003) and most other polar studies (see Garneau et al., 2008 and references therein). Isotope dilution was assumed to be ~ 1 (or negligible, due to low DON concentrations), which is conservative (giving a lower BP per leucine incorporation).

Measurements of BP onboard *Oden* in 2007 were performed similarly, except that the filter method (Kirchman, 2001) was used with ^{14}C-leucine and larger incubation volumes (20 mL).

Size fractionation experiments were run on near surface waters (10–40 m) at Stations 13, 35, 50, and 57 to determine the extent of particle-associated growth. Water was gravity-filtered through a large (293 mm) 3-µm nucleopore filter and measured for BP as described above to determine the contribution to production by free-living bacteria. This value was then compared with the whole water sample and the difference was presumed to account for the production due to particle-associated bacteria.

A temperature sensitivity experiment was run for surface waters at Station 25. Triplicate sets of water samples were processed for BP as above (without size fractionation), but incubated at –1.5, 5, 10, and 20°C.

Total community respiration

Total community respiration (TCR) was measured in the surface (~ 2 m), subsurface (10–40 m), and occasional deep (60–294 m) waters at selected stations (5, 6, 13, 18, 25, 29, 35, 50, 57, 66) and onboard *Oden* in 2007 (Station 16) by examining changes over time of total dissolved inorganic carbon (DIC; see Fransson et al., 2011). Briefly, whole seawater was collected into a sterile 2-L bottle and then dispensed aseptically without bubbling into six identical, sterile, 200-ml pyrex bottles with ground glass stoppers, sealed, and incubated in the dark within 0.5°C of *in situ* temperature. Pairs were fixed by adding 200 µl saturated mercuric chloride solution at 0 h, ~ 24 h and ~ 48 h; bottles were sealed with Apiezon L grease and thick silicone rubber bands, and then stored dark at 2°C until processed in Georgia. Total DIC was measured using a SOMMA and coulometer (Johnson et al., 1993; Cooley and Yager, 2006) with accuracy established using Certified Reference Material and a precision of < 1 µmol C kg^{-1} based on duplicate sample runs (Dickson et al., 2007). Respiration rates were calculated by linear regression using all six points, except when the best linear fit and smallest error was accomplished using only the first four points.

Hydrolysis and extracellular enzyme activity

Bacterial extracellular enzyme activity (EEA) was measured in surface and deep waters at selected stations (13, 14, 35, 50, 57) according to Huston and Deming (2002) to assess the potential for bacterial hydrolysis of particulate organic matter. Four substrates were used: 4-methylumbelliferyl-*N*-acetyl-β-D-glucosaminide (MUF-G; to measure chitobiase activity) and 4-methylumbelliferyl-β-D-glucoside (MUF-B; to measure beta-glucosidase activity), methylumbelliferyl phosphate (MUF-P; to measure alkaline phosphatase activity), and 7-amido-4-methylcoumarin (MCA-L; to measure leucine-aminopeptidase activity). Samples were incubated at 0–2°C and fluorescence was monitored on a Turner fluorometer (TD-400) every 1–2 h until a linear rate was detected (usually ~ 4 h, but up to 72 h for some substrates and samples). An experiment was conducted at Station 57 with surface water from the high-Chl *a* mixed layer (30 m) that examined EEA in four gravity-filtered size fractions: <20 μm, <3 μm, <1 μm, and < 0.2 μm.

Data analysis

With the complex dynamics of changing sea ice cover, wind mixing, and light regime, the polynya displayed a spatial *mosaic* of productivity rather than simple spatial gradients (see Yager et al., 2016). Data were arranged (e.g., Table 1, Figures 2 and 3), therefore, according to the estimated extent of the phytoplankton bloom, as indicated by the integrated DIN depletion (e.g., Yager et al., 2001). This value (ΔDIN_{100}; mmol N m^{-2}) for each station was estimated by integrating total DIN concentrations in the upper 100 m compared to a baseline to determine the amount that had been removed. The winter baseline was determined locally for each station by the concentration of DIN observed at 100 m, which in the ASP was always below the euphotic zone and the base of the summer mixed layer (Tynan, 1998; Prézelin et al., 2000; Yager et al., 2012; Schofield et al., 2015). The ΔDIN_{100} value calculated here does not include several corrections made by Yager et al. (2016) to account for water mass mixing, so we did not convert to carbon units and do not report ΔDIN_{100} as net community production. This value is intended only as a relative measure for viewing microbial data over the bloom progression.

PCA was performed with the 13 environmental variables (year day, latitude, longitude, sample depth, temperature, salinity, DIN, DIP, POC, PON, DOC, DON, and Chl *a*) measured on 79 samples in the upper 100 m of the water column using R statistical analysis software (R Foundation for Statistical Computing, ver. 2.13.2; http://www.r-project.org).

Our method of measuring TCR without pre-filtration (so as not to exclude particle-associated bacteria) meant that the rate also includes dark respiration by phytoplankton and microzooplankton. Thus, bacterial respiration (BR) was conservatively estimated to equal half of TCR, according to Ducklow et al. (2000).

Bacterial carbon demand (BCD) was calculated as BP + BR (Ducklow, 2000; Ducklow et al., 2002). Bacterial growth efficiency (BGE) was calculated as BGE = BP / (BP + BR) (del Giorgio and Cole, 1998).

Correlation coefficients (Pearson's *R*) were calculated according to Sokal and Rohlf (1995), and are reported with the number of paired observations (*n*) and the probability (*p*) of no relationship. Goodness of fit values (R^2) were calculated using linear best-fit regression using reduced major axis (RMA; Sokal and Rohlf, 1995) and Microsoft Excel. All color contour plots were produced using MATLAB statistical analysis software (2012), and the *contour(f)* function. Interpolation between data points was allowed.

Unless otherwise mentioned, all data analyzed are for the upper 100 m water column. If a sample was not collected at exactly 100 m, a value for 100 m was interpolated from data just above and below, and all integrations were done to exactly 100 m. All standard deviations and standard errors of the mean reported were calculated using GraphPad Prism 5 for Windows (ver. 5.04) or Microsoft Excel analysis tools (Microsoft Excel for Macintosh 2011, ver. 14.3.9). When used to indicate variation of observed values across the region, averages reported below include standard deviations (± 1 STD), and the number of samples or rates analyzed (*n*); ranges and medians are reported for non-normal distributions (e.g. counts and small sample sizes). Standard errors (± 1 SE = STD / √n) are used when mean values are directly compared to each other.

Results

Site description and sea ice

ASPIRE sampled the early stages of the 2010–2011 spring bloom (see Figure 1 inset) after the polynya had been open for about one month (Mu et al., 2014). When the ship entered the area on 14 December 2010 the open water area was 41,388 km^2; upon departure from the region on 9 January 2011 it was 72,081 km^2 (see Mu et al., 2014). The open water area peaked at 76,081 km^2 on 12 January 2011, just after we departed. For the 13 stations reported here (Figure 1), eight were in open waters of the central polynya, two (Stations 66 and 68) were in the pack ice, and three (Stations 5, 6, and 34) were under partial sea ice cover (Table 1); sea ice concentration on the sampling date ranged from 0 to 85% (Table 1). The polynya opened first in the southeast and then expanded to the northwest; open water duration ranged from 8 to 61 days (Table 1).

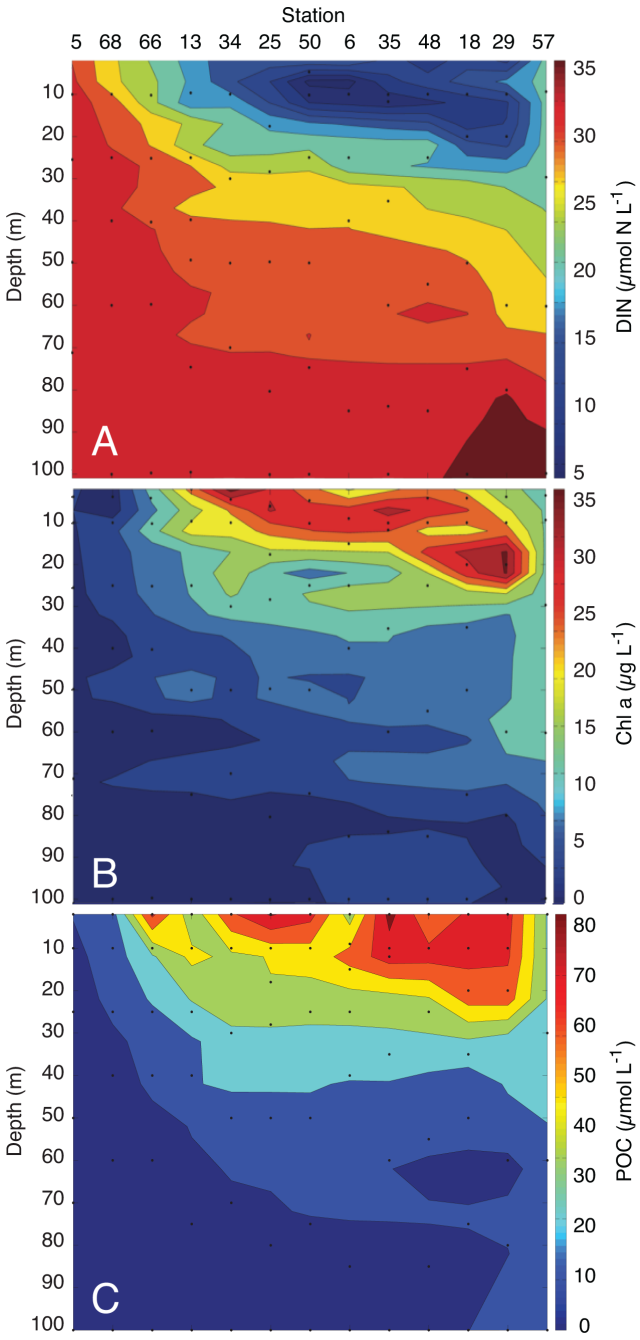

Figure 2

Biogeochemical inventories through the bloom progression.

Biogeochemical inventories versus depth, arranged by station and contoured according to increasing values for integrated nitrogen drawdown (ΔDIN_{100}): A) dissolved inorganic nitrogen (DIN; μmol N L^{-1}); B) chlorophyll *a* (Chl *a*; μg Chl *a* L^{-1}); and C) particulate organic carbon (POC; μmol C L^{-1}).

doi: 10.12952/journal.elementa.000102.f002

Hydrography

Seawater temperature and salinity varied with depth and were strongly associated with specific water masses (mCDW, WW, and Antarctic Surface Water, AASW; Yager et al., 2012; Randall-Goodwin et al., 2015). Waters in the upper 100 m exhibited temperatures ranging from −1.8 to −0.1°C; deeper waters (> 300 m) were warmed (up to ~ 1°C) under the influence of mCDW. The melting of seasonal sea ice, as well as that from icebergs and surrounding ice sheets (see Randall-Goodwin et al., 2015), caused a freshening of surface waters within the ASP (salinities ranged from 33.5 to 34.1 in the upper 100 m), which then led to stratification and warming by the sun. Surface mixed layer depths averaged 25 ± 19 m (Table 1). Strong winds generated deeper upper mixed layers (75–100 m) in some regions to the south nearer to the Dotson Ice Shelf (e.g., Station 57; Figure 1).

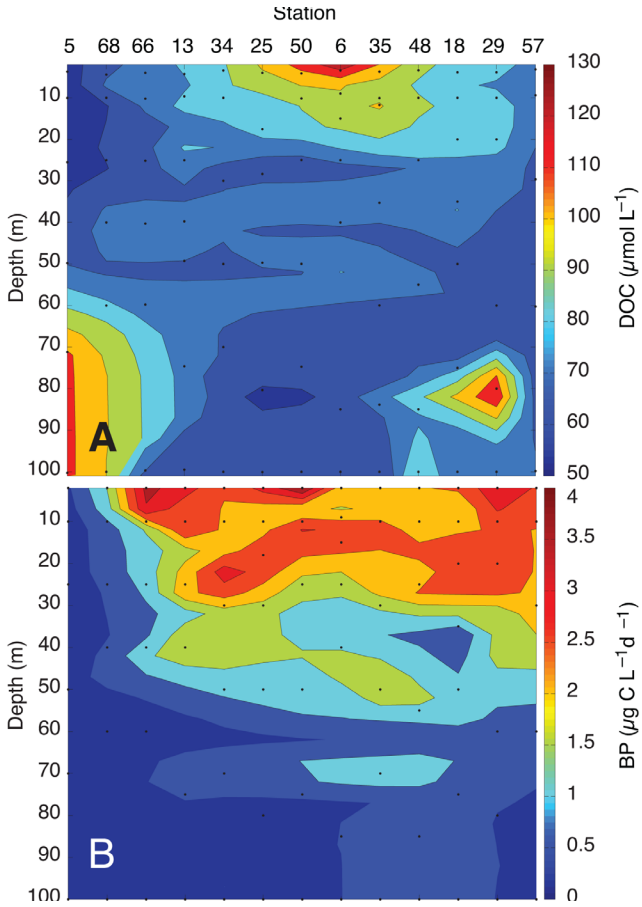

Figure 3

Dissolved substrate inventories and bacterial production through the bloom.

Organic substrate and bacterial activity versus depth arranged by station and contoured according to increasing integrated nitrogen drawdown (ΔDIN_{100}): A) dissolved organic carbon (DOC; μmol C L^{-1}), and B) bacterial production (BP; μg C $L^{-1}d^{-1}$).

doi: 10.12952/journal.elementa.000102.f003

Nutrients

Dissolved inorganic nitrogen (DIN) in the upper 100 m ranged from 7.3 to 31.8 μmol N L^{-1} and was dominated by nitrate; ammonium was < 2 μmol L^{-1} (typically < 1 μmol L^{-1}) and nitrite was < 0.14 μmol N L^{-1}. The highest DIN values were found near the surface at Station 5 and in deeper water (80–100 m) at Stations 29, 57, and 66 (Figure 2A). The lowest DIN concentrations (< 10 μmol N L^{-1}) were found in the upper mixed layer (0–20 m) of Stations 6, 35, and 50; Figure 2A), so we refer to these stations as "peak bloom," even though the regional bloom (as detected by satellite) likely continued for a few more weeks. Winter baseline values for DIN at 100 m ranged from 28.4 to 31.8 (average 29.9 ± 0.93; n = 13) μmol N L^{-1}.

Integrated nitrate depletion (ΔDIN_{100}) ranged from 58 to 740 mmol N m^{-2} (Table 1); it correlated significantly with longitude (R = 0.70; n = 13; p < 0.01) and sea ice concentration (R = −0.59; n = 13; p < 0.05) at the time of sampling (Table 1). These trends reflect the overall pattern of the polynya opening (from southeast to northwest; Stammerjohn et al., 2015) that resulted in larger blooms to the east at the time we sampled, particularly at the open-water stations (Stations 25, 29, 35, 50, 57) compared to ice-edge or marginal ice zone stations to the west (5, 66, 68).

When profiles were arranged in order of bloom extent (ΔDIN_{100}), DIN concentrations exhibited a clear pattern of starting high throughout the upper water column and then showing reductions first near the surface and then moving to depth with increasing ΔDIN_{100} (Figure 2A). Station 57 deviated from the pattern by having the greatest ΔDIN_{100}, but also reflecting the impact of extensive surface wind mixing that increased DIN concentrations near the surface.

Chlorophyll a and NPP

Chlorophyll *a* concentrations in the upper 100 m ranged from 0.02 to 21.8 μg Chl *a* L^{-1}, decreased significantly with depth (R = −0.67; n = 79; p < 0.01), were highest within the surface or near-surface waters of the central polynya, and exhibited a buildup that mirrored the pattern of DIN depletion (Figure 2B; R = −0.89; n = 79; p < 0.01). A subsurface maximum was observed at Stations 18 and 29. Integrated Chl *a* values for the upper

100 m ranged from 70 to 830 mg Chl *a* m^{-2} (Table 1). These integrated values also correlated significantly (R = 0.82; n = 13; $p < 0.01$) with ΔDIN_{100}. Surface wind mixing at Station 57 appears to have dispersed the surface bloom to depth and decreased the Chl *a* concentration at the surface despite peak ΔDIN_{100}.

Net primary production (NPP) ranged from 3 to 104 μg C L^{-1} d^{-1} (median = 14; n = 83), with the highest values (> 60 μg C L^{-1} d^{-1}) found for 0–10 m at open water station (Stations 13, 34, 50, 6, 35, 18, 29) throughout the bloom sequence (see Yager et al., 2016 for full details).

Particulate organic matter

Particulate organic carbon (POC) concentrations in the upper 100 m followed a similar pattern to that of DIN and Chl *a* (Figure 2C), and were highest in the upper 30 m of the central polynya, exceeding 70 μmol C L^{-1} at some stations (e.g., Station 35). Surface wind mixing at Station 57 similarly seems to have also dispersed the POC to depth and decreased the POC concentration at the surface. Points of high POC concentration corresponded positively with Chl *a* maxima (R = 0.90, n = 79; $p < 0.01$), with the POC:Chl *a* ratios for individual samples ranging from 5.6 to 271 (median = 45; n = 66). The handful of extremely high POC:Chl *a* values likely reflect measurement precision as they were only found where total Chl *a* concentrations were relatively low (< 1.5 μg L^{-1}). Particulate organic nitrogen concentrations showed a very similar distribution as POC (R = 0.98; n = 79; $p < 0.01$; Yager et al., 2016), with POC:PON ratios from individual samples averaging 7.1 ± 2.1 (median = 6.8; n = 66).

Dissolved organic matter

Dissolved organic carbon (DOC) concentration in the upper 100 m of the stations ranged from 53 to 127 μmol L^{-1} (Figure 3A) and did not follow the bloom pattern as well as POC described above. There was a general trend of higher DOC (> 100 μmol kg^{-1}) in the surface waters at central polynya stations. While dissolved organic nitrogen (DON) concentrations were relatively low at most stations (below detection to 9 μmol L^{-1}; Yager et al., 2016), there was a trend of higher concentrations in the surface and subsurface at high productivity stations. The correlation between DOC and DON on individual samples was weak but significant (R = 0.39; n = 80; $p < 0.01$). DOC:DON ratios in the upper 100 m of the stations ranged from 9 to 451 (median = 31; n = 69). Some stations showed a DOC spike at depth (70–100 m), without a corresponding DON increase.

Principal component analysis

Results described above suggested that many of the physical and biogeochemical variables co-varied. A PCA generated four principal component axes that explained 82% of the variance (Table 2; Figure 4). PC1 (52% of variance; Table 2) reflected the bloom progression, was positively correlated with DIN (R = 0.98), DIP (R = 0.98), and depth (R = 0.79), and negatively correlated with POC (R = –0.97), PON (R = –0.94), Chl *a* (R = –0.91), DON (R = –0.61), and DOC (R = –0.52). PC2 (15% of variance) correlated with Year day (R = 0.85) and latitude (R = 0.79), and distinguished the more sea-ice-covered stations in the northwest (e.g., Stations 66 and 68) from the others (Figure 4). PC3 (8.1% of variance) reflected non-bloom-associated variations in salinity (R = –0.62) and DOC (R = –0.55). PC4 (6.5% of variance) included additional effects of longitude (R = 0.54) likely associated with the polynya tending to open from east to west.

Table 2. Matrix loading scores for the first four principal components explaining 82% of environmental variance

Parameter	PC 1 (52%)	PC 2 (15%)	PC 3 (8.1%)	PC 4 (6.5%)
DIN	**0.98**	–0.025	0.049	–0.052
DIP	**0.98**	–0.069	0.002	–0.074
POC	**–0.97**	–0.012	–0.034	0.092
PON	**–0.94**	0.006	0.010	0.10
Chl *a*	**–0.91**	–0.12	0.035	0.051
Temperature	**–0.86**	0.046	0.15	–0.033
Depth	**0.79**	–0.20	–0.15	0.17
DON	**–0.61**	–0.15	–0.43	0.005
Year day	0.002	**0.85**	–0.030	0.21
Latitude	0.13	**0.79**	–0.13	0.44
Longitude	–0.31	**–0.55**	0.33	**0.54**
Salinity	0.35	–0.40	**–0.62**	0.40
DOC	–0.52	0.067	**–0.55**	0.32

doi: 10.12952/journal.elementa.000102.t002

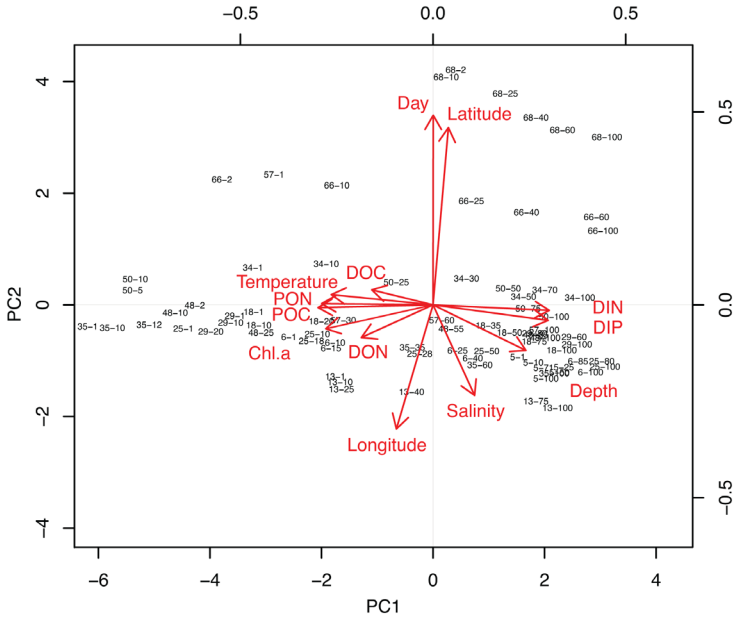

Figure 4

Principal component analysis.

Distance biplot of principal components PC1 vs PC2. Grey numbers correspond to ASPIRE station numbers and depth. Red arrows show the loading of each environmental variable. All values shown are for the upper 100 meters.

doi: 10.12952/journal.elementa.000102.f004

Microbial abundances

Bacterial abundance ranged from 0.1 to 4.0 x 10^9 cells L^{-1} in the upper 100 m of the stations (median = 3 x 10^8 cells L^{-1}). However, one station (Station 68) in the marginal ice zone at the outer shelf break, exhibited significantly elevated abundances (2.4 ± 0.5 x 10^9 cells L^{-1}; n = 6) compared to all of the other stations (3.4 ± 0.2 x 10^8 cells L^{-1}; n = 71) and was assumed to be erroneous. Parallel counts for Station 68 from Swedish collaborators at two depths in the upper 25 m (2 x 10^8 cells L^{-1}) confirmed this error, so we did not use these data further.

Bacterial abundance correlated well with PC2 (R = 0.62; n = 76; $p < 0.01$). When converted to carbon, total integrated bacterial biomass ranged from 36 to 123 mmol C m^{-2} (average = 58 ± 29 mmol C m^{-2}; Table 1) but did not show significant correlations with either ΔDIN_{100} or integrated Chl a (R = 0.29 and 0.02, respectively; n = 12; $p > 0.05$)

Viruses were abundant throughout the upper 100 m of the water column and ranged from 0.1 to 8.2 x 10^9 particles L^{-1} (median = 2.8 x 10^9). They correlated significantly with PC1 (R = −0.44, respectively; n = 30; $p < 0.05$) and also bacterial abundance (R = 0.47; n = 32; $p < 0.01$). Ratios of viruses to bacteria ranged from 0.3 to 24 (median = 8.1), with higher ratios tending to occur later in the bloom progression.

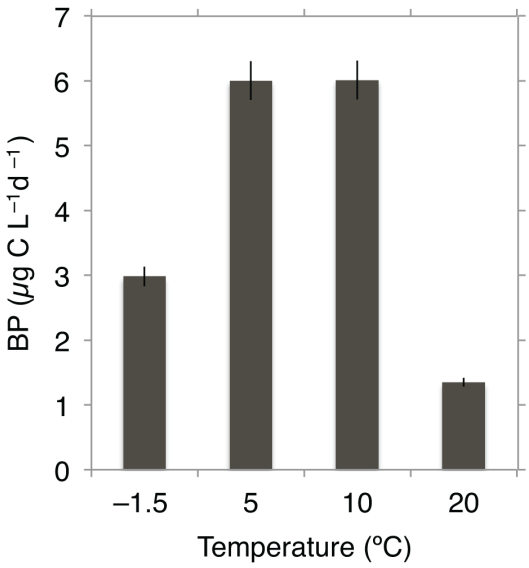

Figure 5

Temperature response of bacterial production.

Bacterial production (BP) in surface waters from Station 25 according to incubation temperature, showing a classic psychrophilic response. Error bars show standard deviations of the mean from triplicate measurements.

doi: 10.12952/journal.elementa.000102.f005

Microzooplankton abundances were low throughout the ASP, with flagellates ranging from 1.1 to 11 x 10^5 cells L^{-1} (median = 4.2 x 10^5 L^{-1}) and ciliates ranging from 0.01 to 5.6 x 10^4 cells L^{-1} (median = 1.9 x 10^4 L^{-1}). Flagellate abundance correlated significantly with PC1 (R = –0.70; n = 30; $p < 0.05$). Ciliates were most abundant at sea-ice-covered Stations 66 and 68, with higher values also observed at Station 57. They did not correlate well with PC1, but showed significant relationships with PC2, PC3, and PC4 (R = 0.55, 0.57 and –0.57, respectively; n = 20; $p < 0.01$).

Microbial activity

Bacterial production (BP; Figure 3B) in the upper 100 m ranged from 0.04 to 4.0 µg C L^{-1} d^{-1} (coefficient of variation on triplicates averaged 14%) and correlated significantly with NPP (R = 0.64; n = 83; $p < 0.01$). BP was greatest in the warmer upper mixed layer, with maximum values in the surface waters at Station 50 (Figure 3B), decreasing rapidly with depth. BP correlated strongly with PC1 (R = –0.88; n = 78; $p < 0.001$), reflecting very tight coupling between bacterial activity and the Chl *a* and POC buildup. The relationship between BP and DOC was relatively weak (as can be seen visually by comparing Figure 3A and 3B) although they were correlated significantly (R = 0.40; n = 71; $p < 0.01$).

Bacterial production also correlated positively with the small increases in *in situ* temperature (R = 0.67; n = 80; $p < 0.01$) observed in the surface waters as the bloom progressed (although this relationship could have been due to covariance with other bloom parameters, as temperature is part of PC1). This possible temperature sensitivity was further examined using short-term warming experiments at Station 25, which indeed showed that BP increased with small increases in temperature, but also showed the classical psychrophilic (cold-loving) temperature response of rates slowing down with too much warming (Figure 4). Warming near-surface waters (18 m) from *in situ* temperature (–1.5°C) to 5°C doubled BP rates (from 3.0 ± 1.1 to 6.0 ± 2.4 µg C L^{-1} d^{-1}), giving a Q_{10} value (Segel, 1975) of 3, slightly higher than the typical Q_{10} of 2 (Kirchman and Rich, 1997). Warming to 10°C did not increase BP further (6.1 ± 2.3 µg C L^{-1} d^{-1}), however, and BP dropped significantly below *in situ* rates when samples were warmed to 20 °C (1.3 ± 0.5 µg C L^{-1} d^{-1}).

Size fractionation experiments conducted at four open water stations (13, 35, 57, and 50) showed that particle-associated activity tended to be higher as POC increased (Figure 6). Particle-associated activity was a small component (10%) of the total BP during the early stages of the bloom (Station 13). At Station 35, when POC was > 60 µmol C L^{-1}, particle-associated activity accounted for about half of the total BP. At peak POC and BP, particle-association accounted for a large fraction (~ 72%) of the total: whole water BP (4.0 ± 1.5 µg C L^{-1} d^{-1}) was significantly higher than that measured on the 3-µm filtered water sample (1.0 ± 0.34 µg C L^{-1} d^{-1}). After the mixing at Station 57, when surface POC dropped below 30 µmol C L^{-1}, particle-associated activity dropped back to about half of the total BP, even though the bloom extent (ΔDIN_{100}) was greatest at Station 57.

Integrated BP ranged from 1.8 to 18 mmol C m^{-2} d^{-1} (Table 1) and showed significant correlation with ΔDIN_{100} and integrated Chl *a* (R = 0.74 and 0.81, respectively; n = 13; $p < 0.01$), but did not correlate significantly with bacterial abundance (R = –0.09; n = 12; $p > 0.05$).

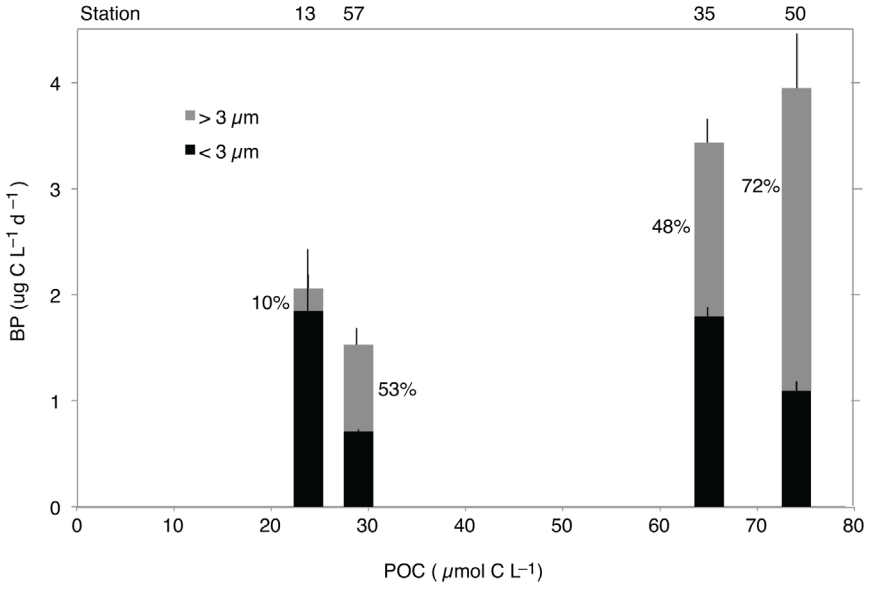

Figure 6

Particle-associated bacterial production.

Particle-associated activity in surface waters from four central polynya stations (13, 57, 35, and 50) with increasing concentration of particulate organic carbon (POC; µmol C L^{-1}). Bacterial production was determined for two size fractions: < 3 µm (black) and > 3 µm (gray). Error bars show standard deviations of the mean from triplicate measurements. Percentages indicate particle association.

doi: 10.12952/journal.elementa.000102.f006

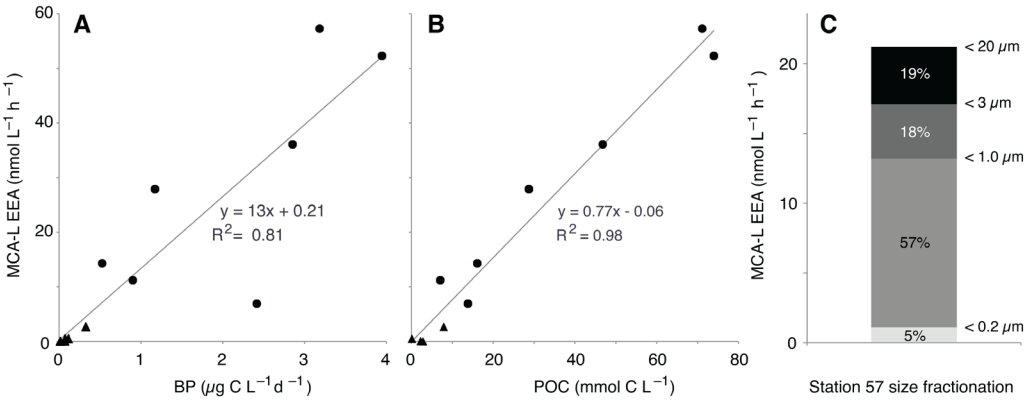

Figure 7

Particle-associated extracellular enzyme activity.

Extracellular enzyme activity (EEA) on MCA-leucine as a function of: A) bacterial production (μg C L^{-1} d^{-1}), B) POC (mmol C L^{-1}), and C) size fraction in surface waters at Station 57. Data in A) and B) derive from both surface (0–100 m; circles) and deep (100–1000 m; triangles) waters at Stations 13, 14, 35, 50, 57.

doi: 10.12952/journal.elementa.000102.f007

Extracellular enzyme activity

Particle-associated growth required bacteria to use extracellular enzymes to convert POM to DOM that could be transported across their cell membranes. Hydrolysis of each of the fluorescent substrates proceeded in linear fashion over the time course of the experiments (data not shown). Of the four enzymes examined here, leucine-aminopeptidase had the highest rates by far (67–249 nmol L^{-1} h^{-1}; median = 36) in the upper 100 m, with maximum rates observed at Station 13. Chitobiase, glucosidase, and alkaline phosphatase activities were all low, with averages (n = 9) of 0.261 ± 0.149, 0.358 ± 0.246, and 0.333 ± 0.335 nmol L^{-1} h^{-1}, in the upper 100 m, respectively. When all depths were included (0–1000 m), leucine-aminopeptidase activity showed significant correlations with BP (R = 0.47; n = 17; $p < 0.01$) and Chl *a* (R = 0.55; n = 19; $p < 0.01$), but the relationship with POC was weak (R = 0.25; n = 16; $p > 0.05$). We noted, however, that two EEA values from surface waters at Station 13 were very high relative to the other data. When these two data points were excluded, the EEA correlations with BP (Figure 7A) and Chl *a* strengthened greatly (R = 0.75 and 0.96, respectively) and POC correlated significantly (R = 0.96; n = 14; $p < 0.01$; Figure 7B).

Size fractionated leucine-aminopeptidase activity at Station 57 showed that a majority of EEA (57%) was cell-associated (0.2–1 μm), with most of the rest of the activity evenly split (18–19% each) between the two particle-associated size classes (1–3 μm and 3–20 μm), and just a small contribution (5%) from the dissolved (< 0.2 μm) fraction (Figure 7). A strong increase in chitobiase, glucosidase, and phosphatase activities (as well as MCA-L) was observed in sinking particles collected in unpoisoned sediment traps (data not shown), suggesting that those extracellular enzymes may be more important to the carbon flux to depth (Ducklow et al., 2015; Yager et al., 2016).

Respiration and growth efficiency

Bacterial respiration (BR) was very high, with rates between 10 and 53 μg C L^{-1} d^{-1}; median = 25; n = 18), although BR did not correlate significantly with BP (R = 0.11; n = 18, $p > 0.05$) or any other single variable. The highest BR was observed in the marginal ice zone at Station 66, but the second highest was late in the bloom progression at Station 57. Such high BR relative to BP contributed to a high BCD (14–57 μg C L^{-1} d^{-1}; median = 27) and a low BGE ranging from 2 to 28% (median = 11). BGE showed a weak relationship with PON (R = 0.52; n = 18; $p < 0.05$).

Sub-euphotic zone microbial abundance and activity

Below the surface 100 m, bacterial numbers declined only slightly (Figure 8A) and microbial activity was dominated by respiration. Over 99% of the integrated bacterial production for each station occurred in the upper 100 m (data > 100 m for all stations not shown). At OSO 2007 Station 16, which had integrated Chl *a* and ΔDIN_{100} values (Table 1) similar to ASPIRE Station 50, bacterial production dropped to undetectable values below 100 m, but bacterial respiration was measurable to 500 m (Figure 8B and C). Integrated subsurface respiration rates for 2007-16 (64 and 60 mmol C m^{-2} d^{-1} for the 100–250 m and 250–500 m horizons, respectively) were comparable to those measured in the surface 0–100 m layer (69 mmol C m^{-2} d^{-1}). With a greater ΔDIN_{100} and POC export potentially enhanced by deep mixing (Yager et al., 2016), ASPIRE Station 57 showed much higher bacterial abundance and respiration at sub-euphotic depths compared to 2007-16. Respiration rates at 300 m were only about 20% lower than those measured at the surface of Station 57 (Figure 8C). The integrated subsurface respiration rate was higher for 100–250 m (545 mmol C m^{-2} d^{-1}) than for the surface 0–100 m (369 mmol C m^{-2} d^{-1}). The activities of sub-euphotic zone bacteria likely remineralize a significant fraction of the sinking flux of particles from the surface bloom (Ducklow et al., 2015).

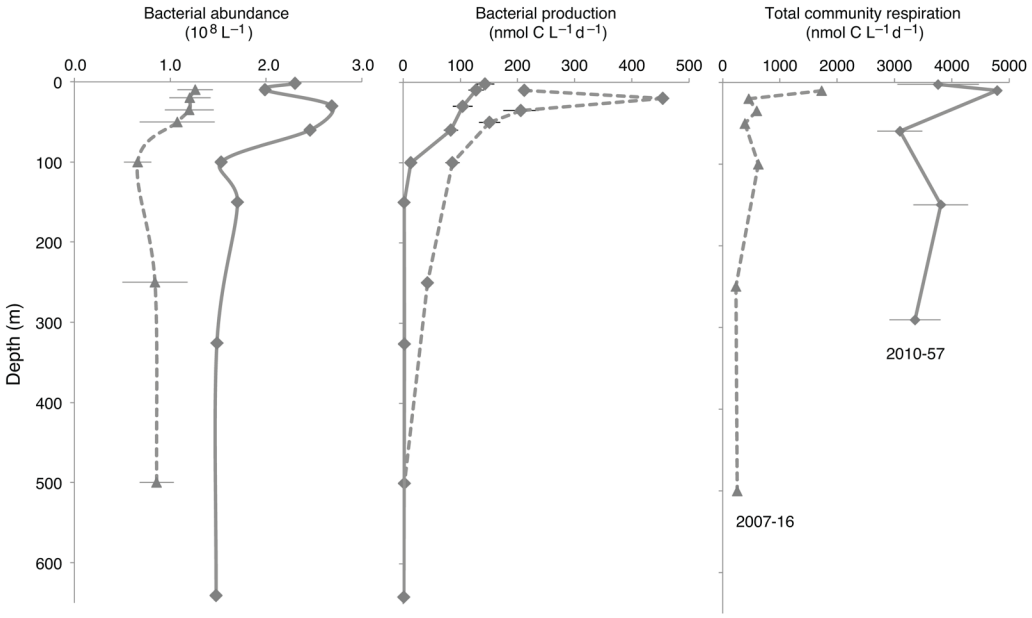

Figure 8

Sub-euphotic zone microbial activity.

Deep profiles for bacterial abundance, bacterial production, and total community respiration at two polynya stations: ASPIRE Station 57 (solid gray) and OSO 2007 Station 16 (dashed gray).

doi: 10.12952/journal.elementa.000102.f008

Heterotrophy versus autotrophy in the ASP

As described above, bacterial growth (BP) was highly correlated with NPP, suggesting that microbial autotrophs and heterotrophs are well-coupled in this system, but the BP:NPP ratio was generally low across all stations (median = 6.1%; n = 83). A reduced major axis regression between BP and NPP showed a linear trend (R^2 = 0.48, $p < 0.01$) at the lower NPP range (< 40 μg C L^{-1} d^{-1}), with a slope of 0.097, but when NPP exceeded 40 μg C L^{-1} d^{-1} the slope of the relationship "saturated", suggesting an uncoupling between BP and NPP at high NPP (Figure 9).

With BR added to BP, however, the bacterial carbon demand (BCD) became more significant relative to primary production. When rates from individual stations and depths were compared to each other directly, BCD:NPP in the ASP was high (median = 80%; ranging from 18 to 300%) and seemingly inconsistent with the greatly undersaturated pCO_2 (Mu et al., 2014) and large NCP (Yager et al., 2016) observed in the upper 100 m. The imbalance was likely a result of measuring the more effort-intensive BR at fewer depths, and primarily at the surface (1–5 m), whereas at 10 of 13 stations NPP was highest just below the surface (10–25 m; see Yager et al., 2016; Schofield et al., 2015). When we measured BR below the surface, or coincident with the NPP maxima, BCD:NPP tended to be lower (median = 29%; n = 8).

To account for vertical mixing then, we estimated BCD for the full water column of each station by applying an average BGE to each BP profile to estimate a full BCD profile. The resulting integrated heterotrophic demand was more in line with integrated NPP (median BCD/NPP = 43%; ranging from 25 to 130%), with the higher ratios coming from later-bloom stations (e.g., Stations 48 and 57) where algal biomass was very high and self-shading was likely causing light limitation *in situ* (Schofield et al., 2015).

Discussion

Regional significance

The ASPIRE observations support the designation of the ASP as one of the most productive bloom systems in the world. During the early stages of the summer bloom in the ASP, Chl *a* concentrations (> 20 μg Chl *a* L^{-1}) and rates of NPP (228 ± 71 mmol C m^{-2} d^{-1}; Yager et al., 2016) were high and comparable to or in excess of maximum concentrations and rates reported elsewhere in the Antarctic coastal ocean (Holm Hansen and Mitchell, 1991; Vernet et al., 2008; Smith et al., 2014), as well as the North Atlantic (Martin et al., 1993) and coastal Arctic (Matrai et al., 2013). Maxima for both primary and secondary production were associated with the lower-salinity, warmer surface waters of the central ASP (for details see Schofield et al., 2015; Yager et al., 2016). NPP correlated significantly with PC1 (R = –0.57; n = 68; $p < 0.001$). Light limitation from self-shading likely impacted rates later in the bloom (Schofield et al., 2015).

BP in the upper 100 m of the ASP (0.2–4 μg C L^{-1} d^{-1}) was comparable to or higher than most of the rates measured in and around the coastal Antarctic, including the Weddell Sea (0.1–7 μg C L^{-1} d^{-1}; Billen and Becquevort, 1990; Vaqué et al., 2002), and yielded higher depth-integrated BP rates (135 ± 49 mg C m^{-2} d^{-1}; Table 1) than all those measured at the Palmer LTER research site between 2003 and 2011 (< 70 mg C m^{-2} d^{-1} across all years and regions; Ducklow et al., 2012). Our conversion factors were chosen

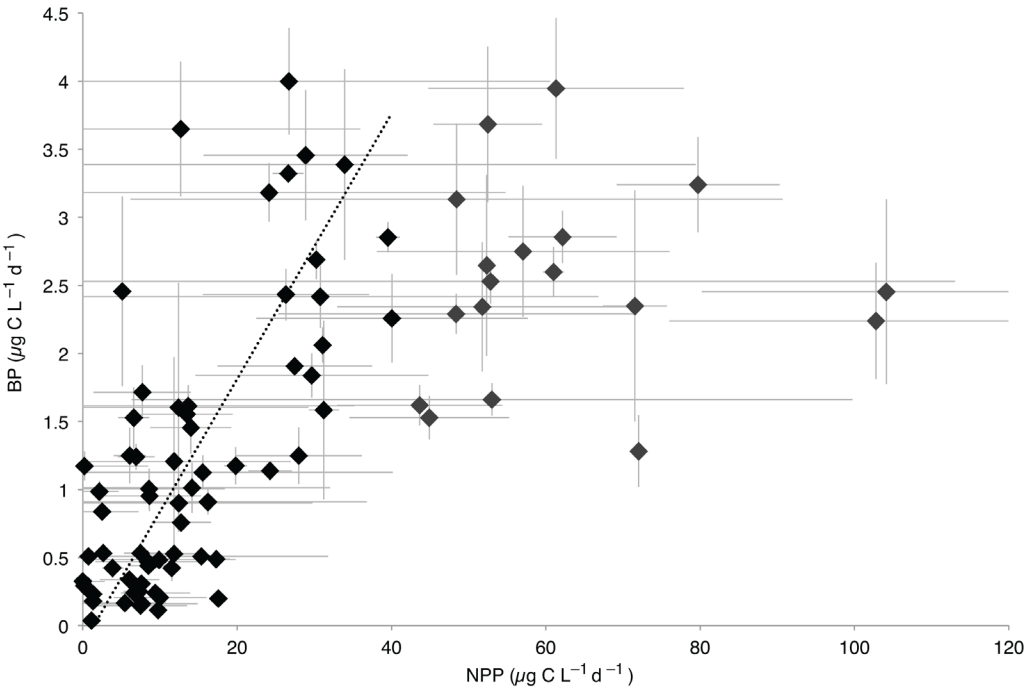

Figure 9

Bacterial production versus net primary production.

Bacterial production (BP; μg C L^{-1} d^{-1}) plotted as a function of net primary production (NPP; μg C L^{-1} d^{-1}) showing the linear response at lower NPP and the saturating response above ~ 40 μg C L^{-1} d^{-1}. Error bars in gray indicate ±1 standard deviation from the mean of triplicate measurements. A Reduced Major Axis (RMA) regression line (slope = 0.097, y-intercept = −0.14, and R^2 = 0.48) is shown (black dashes). All data are from the upper 100 m where NPP rates were measured; dark gray points are above the 40 μg C L^{-1} d^{-1} threshold and were not used in the RMA regression.

doi: 10.12952/journal.elementa.000102.f009

to be conservative, but even when their influence is removed, rates of leucine incorporation in the ASP (0.154–2.59 nmol L^{-1} d^{-1}) were approximately double those reported in the nearby Ross Sea (0.240–0.940 nmol L^{-1} d^{-1}, as calculated from data in Ducklow et al., 1999). Including isotope dilution would further increase BP and BCD. Thus, these regionally high production values within the polynya suggest that the microbial community was highly active and growing in the low, ambient water temperatures (−1.8 to −0.1 °C). Temperature sensitivity experiments indicated the presence of an active psychrophilic community that responded rapidly to a few degrees of warming, implying that it could be responsive to but also possibly vulnerable to future climate change.

What processes support high rates of microbial heterotrophy?

In the Amundsen Sea Polynya, surface algal blooms are dominated by *Phaeocystis antarctica* beginning in December and reach maximum abundance in mid-February (Arrigo and van Dijken, 2003). In the neighboring Ross Sea there is a time lag of approximately one month between the phytoplankton bloom and the bacterial bloom, in part because of the slow release of labile DOC from *Phaeocystis* but also by the low production of DOC through limited grazing (Ducklow, 2003). This delay in the bacterial response is not a result of temperature inhibition (Kirchman et al., 2009), but rather of resource limitation (Carlson et al., 1999), and depends on the inventories of labile and semi-labile DOC (Ducklow et al., 2001; Ducklow and Yager, 2007). We did not detect such a lag in the ASP; BP ramped up with PP during this early part of the summer season. Since the ASP did not exhibit a large buildup of DOM in conjunction with other bloom-associated inventories such as POM and Chl *a* (see also Yager et al., 2016), there must have been either low DOM production or rapid DOM turnover by microbial heterotrophs. The rapid turnover scenario is suggested by the high rates of bacterial production that we observed. Bacteria living in close association with the *Phaeocystis* colonies (e.g., Delmont et al., 2014, 2015), could take up dissolved products directly from the phytoplankton, thus limiting DOM release to the seawater and detection at anything but low levels. A high DOM flux and rapid turnover may also explain high respiration rates and low growth efficiencies if luxury consumption by the bacteria occurs (Kirchman et al., 2009).

In the Ross Sea, about 89% of the organic carbon produced during *Phaeocystis* blooms was shown to be partitioned as POC (Carlson et al., 1998). Indeed, the majority of organic matter in the ASP is probably bound inside *P. antarctica* cells (Schoemann et al., 2005) and cannot be directly utilized by bacteria (Tang et al., 2001) unless the cells are in mutualistic association (e.g., Delmont et al., 2015) as discussed above. Free-living heterotrophic communities, such as those seen during the very early stages of the bloom, rely on phytoplankton extracellular release (PER) of DOM (Billen and Becquevort, 1990) or other processes that convert POM to utilizable DOM. If PER was low in the ASP, then alternate means of supplying DOM to support the observed high rates of bacterial production would include 1) grazing activities, 2) viruses that lyse DOM-rich *P. antarctica,* and 3) extracellular enzymes that breakdown organic matter associated with particle aggregates. These potential sources are discussed below.

Grazing activity and viral lysis

Grazing activities contribute significantly to dissolved and particulate organic matter fluxes in marine environments through sloppy feeding and excreta (Jumars et al., 1989, 1993; Steinberg et al., 2000, 2008). Protozoan and metazoan grazers can play a vital role in microbial loop dynamics (Azam et al., 1983; Sherr and Sherr, 2002; Pomeroy et al., 2007), but large colonies of *Phaeocystis* are not readily grazed by micro- or mesozooplankton (Caron et al., 2000; Nejstgaard et al., 2007). Flagellate and protist abundances were generally low in the upper 100 m of the ASP, as were macrozooplankton abundances in the upper 40 m (Wilson et al., 2015). Low levels of microzooplankton grazers also characterize the neighboring Ross Sea Polynya (Tagliabue and Arrigo, 2003). While these lower grazer abundances would contribute little to DOM production, the lower abundances of microzooplankton may also reduce grazing pressure on the bacteria themselves.

Viral infection can provide another source of DOM to the microbial loop. As algae and bacteria are lysed by viruses, intracellular organic matter is released as labile DOM to the environment where it is available for heterotrophic microbial utilization (Gobler et al., 1997; Middelboe and Jørgensen, 2006). Ratios of viruses to bacteria in the ASP were similar to ratios observed during austral summer in the West Antarctic Peninsula (Karl et al., 1996), during an under-ice algal bloom in the Chukchi Sea (Yager et al., 2001), and in Atlantic surface waters (~ 10), but low compared to Pacific ratios (~ 40; Suttle, 2007). Viral abundances in the ASP correlated best with DON, perhaps reflecting their release in elevated numbers along with nitrogen-rich DOM following host lysis. They also showed a significant correlation with bacterial abundance (excluding Station 68), as earlier observed by Fuhrman (1999), but not with Chl *a*, implying more bacteriophage than phytoplankton viruses in the ASP. Viral interaction with and infection of bacterial communities also reduces BGE (Fuhrman, 1992; Middelboe et al., 1996), and we calculated low BGE in the ASP.

The role of particles

Large aggregates of living or dead organic matter produced during phytoplankton blooms are enriched in organic substrates and thus well known hot-spots for heterotrophic bacterial activities and the turnover of photosynthetically fixed carbon (Simon et al., 2002). The abundance of organic aggregates in the polynya system could partly explain high levels of bacterial activity in the ASP despite low observed DOM concentrations, similar to algal blooms in the Chukchi Sea (Yager et al., 2001; Hodges et al., 2005). In the ASP, BP was found to correlate with both PON and POC, and size-fractionation experiments confirmed variable degrees of particle association in open water stations. Particle association may be indicative of a mutualistic relationship between bacteria and living *Phaeocystis* (Delmont et al., 2014, 2015), of the breakdown of dead or dying phytoplankton via extracellular enzymes, or of a combination of these phenomena. Determining which of these bacteria-particle interactions dominates, temporally and spatially, will be important for understanding the role of pelagic microbial heterotrophs in the carbon cycling of this region. Further analyses of bacterial community structure in the ASP (Kim et al., 2013; Richert et al., 2015) may help to resolve the issue, but it is already clear that bacterial taxa known for particle attachment and copiotrophy (consumption of high levels of DOM) dominate in the epipelagic zone of this polynya (Richert et al., 2015).

The positive correlations between BP, POC, and EEA suggest that bacteria were benefiting from extracellular enzymes (particularly MCA-L) that hydrolyze POM to more labile DOM. Particle association and the production of extracellular enzymes, which is generally more energetically taxing than a free-living lifestyle (Vetter et al., 1998; Deming, 2002), would be favored in a setting with limited sources of dissolved organic matter and reflected in a high fraction of pelagic bacterial respiration, both of which we observed. Bacteria in the ASP were diverting, on average, 91% of total carbon uptake to respiration. One explanation for this finding may be that the particulate matter was of low quality, as found in decaying cells, and provided a less than ideal substrate for bacterial growth. This idea is not supported, however, by the relatively low average POC:PN and POC:Chl *a* ratios in the polynya (7.0 ± 0.81 and 52 ± 20, respectively, n = 13; Yager et al., 2016) throughout this early summer bloom (with no significant relationship to increasing nitrate depletion; Yager et al., 2016). Proteinase activity, which dominated ASP EEA, could be linked to cell-associated utilization of high-molecular weight (HMW) DOM rather than POM, suggested by the high percentage of EEA activity in the 0.2–1.0 μm size fraction. If the free-living bacteria are utilizing bioavailable HMW proteins (N rich) cleaved through EEA, such utilization would require more energy for enzyme production, hence low BGE.

High rates of BP can lead to low BGE when high fluxes of labile DOM are available, as could have been the case with either free-living bacteria or those living in association with the *Phaeocystis* colonies. Tight coupling between autotrophs and heterotrophs, combined with low bacterial growth efficiencies and high BCD, could reduce vertical export potential during the early bloom. Only after NPP exceeded the observed threshold (~ 50 μg C L^{-1} d^{-1}) was there opportunity for an autotroph-to-heterotroph temporal lag. Such a lag would allow for greater potential export from these polar surface waters and would support a more efficient biological pump later in the season. Mesopelagic respiration rates, however, particularly later in the bloom

progression at Sta 57, were high or comparable to other ocean regions such as the summertime North Atlantic (Collins et al. 2015) and could have significantly reduced the amount of fixed carbon sinking to great depth (Ducklow et al., 2015; Yager et al., 2016).

Conclusions

Our estimates of microbial activity in the Amundsen Sea Polynya reveal high rates of bacterial production previously unreported in polar marine systems. Despite relatively high Chl *a* and NPP, observed DOM in the ASP was low; any DOM produced by phytoplankton extracellular release, viral lysis, grazing, or hydrolysis was apparently taken up quickly by the bacteria. Micro- and macro-zooplankton abundances in the upper 40 m were low, suggesting reduced DOM release via grazing, although viral abundance increased with bacterial abundance over the course of the bloom and may have contributed to DOM flux. Rapid DOM turnover in the epipelagic was further suggested by low growth efficiencies indicating luxury consumption. Once the bloom was well underway, particle-associated activities seen at higher particle concentrations, support the idea of either a mutualism between *Phaeocystis* colonies and their heterotrophic bacterial partners, or a particle-associated lifestyle, in conjunction with extracellular enzyme hydrolysis of POM to DOM. Significant findings were that bacterial production was cold-adapted, and that there was no observed lag between bacterial activity and primary production. High bacterial carbon demand in the surface also characterized sub-euphotic depths, supporting other estimates of rapid mesopelagic remineralization of sinking particles from the bloom.

References

Alderkamp AC, Dijken GL, Lowry KE, Connelly TL, Lagerstrom M, et al. 2015. Fe availability drives phytoplankton photosynthesis rates during spring bloom in the Amundsen Sea Polynya, Antarctica. *Elem Sci Anth* **2**: 000043 doi: 10.12952/journal.elementa.000043.

Alderkamp AC, Mills MM, Van Dijken GL, Laan P, Thuyróczy CE, et al. 2012. Iron from melting glaciers fuels phytoplankton blooms in the Amundsen Sea (Southern Ocean): Phytoplankton characteristics and productivity. *Deep-Sea Res Pt II* **71–76**: 32–48. doi: 10.1016/j.dsr2.2012.03.005.

Arrigo KR, Lowry KE, van Dijken GL. 2012. Annual changes in sea ice and phytoplankton in polynyas of the Amundsen Sea, Antarctica. *Deep-Sea Res Pt II* **71–76**: 5–15. doi: 10.1016/j.dsr2.2012.03.006.

Arrigo KR, Robinson DH, Worthen DL, Dunbar RB, DiTullio GR, et al. 1999. Phytoplankton community structure and the drawdown of nutrients and CO_2 in the Southern Ocean. *Science* **283**: 365–367.

Arrigo KR, van Dijken GL. 2003. Phytoplankton dynamics within 37 Antarctic coastal polynya systems. *J Geophys Res* **108**: 3271. doi: 10.1029/2002JC001739.

Arrigo KR, van Dijken GL, Bushinsky S. 2008. Primary production in the Southern Ocean, 1997–2006. *J Geophys Res* **113**: C08004. doi: 10.1029/2007JC004551.

Arrigo KR, van Dijken GL, Strong A. 2015. Environmental controls of marine productivity hot-spots around Antarctica. *J Geophys Res.* **120**(8): 5545–5565. doi: 10.1002/2015JC010888.

Azam F, Field JG, Gray JS, Meyer-Reil LA, Thingstad F. 1983. The ecological role of water-column microbes in the sea. *Mar Ecol-Prog Ser* **10**: 257–263.

Billen G, Becquevort S. 1990. Phytoplankton – bacteria relationship in the Antarctic marine ecosystem. *Polar Res* **10**(1): 245–253.

Buesing N, Gessner MO. 2003. Incorporation of radiolabeled leucine into protein to estimate bacterial production in plant litter, sediment, epiphytic biofilms, and water samples. *Microb Ecol* **45**: 291–301.

Carlson CA, Bates NR, Ducklow HW, Hansell DA. 1999. Estimation of bacterial respiration and growth efficiency in the Ross Sea, Antarctica. *Aquat Microb Ecol* **19**: 229–244.

Carlson CA, Ducklow HW, Hansell DA, Smith WO. 1998. Organic carbon partitioning during spring phytoplankton blooms in the Ross Sea polynya and the Sargasso Sea. *Limnol Oceanogr* **43**: 375–386.

Caron DA, Dennett MR, Lonsdale DJ, Moran DM, Shalapyonok L. 2000. Microzooplankton herbivory in the Ross Sea, Antarctica. *Deep-Sea Res Pt II* **47**: 3249–3272.

Christaki U, Courties C, Massana R, Catala P, Lebaron P, et al. 2011. Optimized routine flow cytometric enumeration of heterotrophic flagellates using SYBR Green I. *Limnol Oceanogr: Methods* **9**: 329–339.

Collins JR, Edwards BR, Thamatrakoln K, Ossolinski JE, DiTullio GR, et al. 2015. The multiple fates of sinking particles in the North Atlantic Ocean. *Global Biogeochem Cy* **29**: 1471–1494. doi: 10.1002/2014GB005037.

Cooley SR, Yager PL. 2006. Physical and biological contributions to the western tropical North Atlantic Ocean carbon sink formed by the Amazon River plume. *J Geophys Res* **111**: C08018. doi: 10.1029/2005JC002954.

del Giorgio PA, Cole JJ. 1998. Bacterial growth efficiency in natural aquatic systems, in Kirchman DL, Microbiology WSIEADA, eds., *Microbial Ecology of the Oceans*. New York: Wiley-Liss: pp. 289–325.

Delmont TO, Eren AM, Vineis JH, Post AF. 2015. Genome reconstructions indicate the partitioning of ecological functions inside a phytoplankton bloom in the Amundsen Sea, Antarctica. *Front Microbiol* **6**: 1090. doi: 10.3389/fmicb.2015.01090.

Delmont TO, Hammar KM, Ducklow HW, Yager PL, Post AF. 2014. *Phaeocystis antarctica* blooms strongly influence bacterial community structures in the Amundsen Sea polynya. *Front Microbiol* **5**: 646. doi: 10.3389/fmicb.2014.00646.

Deming JW. 2002. Psychrophiles and polar regions. *Curr Opin Microbiol* **5**: 301–309.

Dickson AG, Sabine CL, Christian JR. 2007. Guide to best practices for ocean CO_2 measurements. Sidney, British Columbia: North Pacific Marine Science Organization. *(PICES Special Publication 3)* 176 pp.

Dolan JR, Yang EJ, Lee SH, Kim SY. 2013. Tintinnid ciliates of Amundsen Sea (Antarctica) plankton communities. *Polar Res* **32**: 19784.

Dubnick A, Barker J, Sharp M, Wadham J, Grzegorz L, et al. 2010. Characterization of dissolved organic matter (DOM) from glacial environments using total fluorescence spectroscopy and parallel factor analysis. *Ann Glaciol* **51**(56): 111–122.

Ducklow HW. 2000. Bacterial production and biomass in the oceans, in Kirchman DL ed., *Microbial Ecology of the Oceans*. New York: Wiley-Liss: pp. 85–120.

Ducklow HW. 2003. Seasonal production and bacterial utilization of DOC in the Ross Sea, Antarctica, in Ditullio GR, Dunbar RB, eds., *Biogeochemistry of the Ross Sea*. Washington, D.C.: American Geophysical Union. doi: 10.1029/078ARS09.

Ducklow HW, Carlson CA, Church M, Kirchman DL, Smith D, et al. 2001. The seasonal development of the bacterioplankton bloom in the Ross Sea, Antarctica, 1994–1997. *Deep-Sea Res Pt II* **48**(19–20): 4199–4221.

Ducklow HW, Carlson CA, Smith Jr WO. 1999. Bacterial growth in experimental plankton assemblages and seawater cultures from the *Phaeocystis antarctica* bloom in the Ross Sea, Antarctica. *Aquat Microb Ecol* **19**: 215–227.

Ducklow HW, Dickson ML, Kirchman DL, Steward G, Orchardo J, et al. 2000. Constraining bacterial production, conversion efficiency and respiration in the Ross Sea, Antarctica, January-February, 1997. *Deep-Sea Res Pt II* **47**: 3227–3247.

Ducklow HW, Fraser WR, Meredith MP, Stammerjohn SE, Doney SC, et al. 2013. West Antarctic Peninsula: An ice-dependent coastal marine ecosystem in transition. *Oceanogr* **26**(3): 190–203. doi: 10.5670/oceanog.2013.62.

Ducklow HW, Kirchman DL, Anderson TR. 2002. The magnitude of spring bacterial production in the North Atlantic Ocean. *Limnol Oceanogr* **47**(6): 1684–1693.

Ducklow HW, Kirchman DL, Quinby HL. 1992. Bacterioplankton cell growth and macromolecular synthesis in seawater cultures during the North Atlantic Spring Phytoplankton Bloom, May 1989. *Microb Ecol* **24**(2): 125–144. doi: 10.1007/BF00174450.

Ducklow HW, Schofield O, Vernet M, Stammerjohn S, Erickson M. 2012. Multiscale control of bacterial production by phytoplankton dynamics and sea ice along the western Antarctic Peninsula: A regional and decadal investigation. *J Mar Syst* **98–99**: 26–39 doi: 10.1016/j.jmarsys.2012.03.003.

Ducklow HW, Wilson SE, Post AF, Stammerjohn SE, Erickson M, et al. 2015. Particle flux on the continental shelf in the Amundsen Sea Polynya and Western Antarctic Peninsula. *Elem Sci Anth* **3**: 000046. doi: 10.12952/journal.elementa.000046.

Ducklow HW, Yager PL. 2007. Pelagic Bacterial Processes in Polynyas, in Smith Jr WO, Barber D, eds., *Polynyas: Windows into Polar Oceans*. Elsevier Oceanography Series: pp 323–361.

Feng X, Vonk JE, van Dongen BE, Gustafsson O, Semiletov IP, et al. 2013. Differential mobilization of terrestrial carbon pools in Eurasian Arctic river basins. *P Natl Acad Sci* **110**(35): 14,168–14,173.

Fransson A, Chierici M, Yager PL, Smith Jr WO. 2011. Antarctic sea ice carbon dioxide system and controls. *J Geophys Res* **116**: C12035. doi: 10.1029/2010JC006844.

Fuhrman JA. 1992. Bacterioplankton roles in cycling of organic matter: The microbial food web, in Falkowski PG, Woodhead AD, Vivirito K, eds., *Primary Productivity and Biogeochemical Cycles in the Sea*. United States: Springer. Vol. **43**: pp. 361–383. doi: 10.1007/978-1-4899-0762-2_20.

Fuhrman JA. 1999. Marine viruses and their biogeochemical and ecological effects. *Nature* **399**: 541–548. doi: 10.1038/21119.

Garneau MÈ, Roy S, Lovejoy C, Gratton Y, Vincent WF. 2008. Seasonal dynamics of bacterial biomass and production in a coastal arctic ecosystem: Franklin Bay, western Canadian Arctic waters. *J Geophys Res* **113**. doi: 10.1029/2007JC004281.

Gobler CJ, Hutchins DA, Fisher NS, Cosper EM, Sañudo-Wilhelmy SA. 1997. Release and bioavailability of C, N, P, Se, and Fe following viral lysis of a marine chrysophyte. *Limnol Oceanogr* **42**(7): 1492–1504

Goswami SC. 2004. Zooplankton methodology, collection & identification -a field manual. National Institute of Oceanography. Dona Paula, Goa: 26 pp.

Hodges LR, Bano N, Hollibaugh JT, Yager PL. 2005. Illustrating the importance of particulate organic matter to pelagic microbial abundance and community structure—an Arctic case study. *Aquat Microb Ecol* **40**(3): 217–227. doi: 10.3354/ame040217.

Holm-Hansen O, Mitchell BG. 1991. Spatial and temporal distribution of phytoplankton and primary production in the western Bransfield Strait region. *Deep-Sea Res Pt I* **38**(8/9): 961–980.

Huston AL, Deming JW. 2002. Relationships between microbial extracellular enzymatic activity and suspended and sinking particulate organic matter: Seasonal transformations in the North Water. *Deep-Sea Res Pt II* **49**(22–23): 5211–5225.

Johnson KM, Wills KD, Butler DB, Johnson WK, Wong CS. 1993. Coulometric total carbon dioxide analysis for marine studies: Maximizing the performance of an automated gas extraction system and coulometric detector. *Mar Chem* **44**: 167–187.

Jumars PA, Deming JW, Hill PS, Karp-Boss L, Yager PL, et al. 1993. Physical constraints on marine osmotrophy in an optimal foraging context. *Mar Microb Food Webs* **7**(2): 121–159.

Jumars PA, Penry DL, Baross JA, Perry MJ, Frost BW. 1989. Closing the microbial loop: Dissolved carbon pathway to heterotrophic bacteria from incomplete digestion, digestion, and absorption in animals. *Deep-Sea Res Pt I* **36**(4): 483–495.

Karl DM, Christian JR, Dore JE. 1996. Microbiological oceanography in the region west of the Antarctic Peninsula: Microbial dynamics, nitrogen cycle, and carbon flux. *Antarct Res Ser* **70**: 303–332.

Kennedy F, McMinn A, Martin A. 2012. Effect of temperature on the photosynthetic efficiency and morphotype of Phaeocystis antarctica. *J Exp Mar Biol Ecol* **429**: 7–14. doi: 10.1016/j.jembe.2012.06.016.

Kim JG, Park SJ, Quan ZX, Jung MY, Cha IT, et al. 2013. Unveiling abundance and distribution of planktonic *Bacteria* and *Archaea* in a polynya in Amundsen Sea, Antarctica. *Environ Microbiol*. doi: 10.1111/1462-2920.12287.

Kirchman DL. 2001. Measuring bacterial biomass production and growth rates from leucine incorporation in natural aquatic environments, in Paul JH ed., *Methods in Microbiology*. Vol. 30. Marine Microbiology. San Diego: Academic Press. pp. 227–237.

Kirchman DL, K'nees E, Hodson R. 1985. Leucine incorporation and its potential as a measure of protein synthesis by bacteria in natural aquatic systems. *Appl Environ Microb* **49**(3): 599–607.

Kirchman DL, Morán XAG, Ducklow HW. 2009. Microbial growth in the polar oceans - role of temperature and potential impact of climate change. *Nature Rev Microb* **7**: 451–459.

Kirchman DL, Rich JH. 1997. Regulation of bacterial growth rates by dissolved organic carbon and temperature in the equatorial Pacific Ocean. *Microb Ecol* **33**(1): 11–20.

Knap A, Michaels A, Close A, Ducklow HW, Dickson A. 1996. Protocols for the Joint Global Ocean Flux Study (JGOFS) Core Measurements. *JGOFS Report No. 19. Reprint of the IOC Manuals and Guides No. 29*. UNESCO.

Marie D, Brussaard CPD, Thyrhaug R, Bratbak G, Vaulot D. 1999. Enumeration of marine viruses in culture and natural samples by flow cytometry. *Appl Environ Microbiol* **65**(1): 45–52.

Marie D, Partensky F, Jacquet S, Vaulot D. 1997. Enumeration and cell cycle analysis of natural populations of marine picoplankton by flow cytometry using the nucleic acid stain SYBR Green I. *Appl Environ Microb* **63**(1): 186–193.

Martin JH, Fitzwater SE, Gordon RM. 1990. Iron deficiency limits phytoplankton growth in Antarctic waters. *Global Biogeochem Cy* **4**(1): 5–12. doi: 10.1029/GB004i001p00005.

Martin JH, Fitzwater SE, Gordon RM, Hunter CN, Tanner SJ. 1993. Iron, primary production and carbon-nitrogen flux studies during the JGOFS North Atlantic bloom experiment. *Deep-Sea Res Pt II* **40**(1): 115–134.

Matrai PA, Olson E, Suttles S, Hill V, Codispoti LA, et al. 2013. Synthesis of primary production in the Arctic Ocean: I. Surface waters, 1954–2007. *Progr Oceanogr* **110**: 93–106. doi: 10.1016/j.pocean.2012.11.004.

Middelboe M, Jørgensen NOG. 2006. Viral lysis of bacteria: An important source of dissolved amino acids and cell wall compounds. *J Mar Biol Assoc UK*. **86**: 605–612

Middelboe M, Jørgensen NOG, Kroer N. 1996. Effects of viruses on nutrient turnover and growth efficiency of noninfected marine bacterioplankton. *Appl Environ Microbiol* **62**(6): 1991–1997.

Montes-Hugo M, Doney SC, Ducklow HW, Fraser W, Martinson D, et al. 2009. Recent changes in phytoplankton communities associated with rapid regional climate change along the western Antarctic Peninsula. *Science* **323**(5920): 1470–1473

Mu L, Stammerjohn SE, Lowry KE, Yager PL. 2014. Spatial variability of surface pCO_2 and air-sea CO_2 flux in the Amundsen Sea Polynya, Antarctica. *Elem Sci Anth.* **2**: 000036. doi: 10.12952/journal.elementa.000036.

Nejstgaard JC, Tang KW, Steinke M, Dutz J, Koski M, et al. 2007. Zooplankton grazing on *Phaeocystis*: A quantitative review and future challenges. *Biogeochemistry* **83**: 147–172.

Nitsche FO, Jacobs S, Larter RD, Gohl K. 2007. Bathymetry of the Amundsen Sea continental shelf: Implications for geology, oceanography, and glaciology. *Geochem Geophys Geosys* **8**: Q10009. doi: 10.1029/2007GC001694.

Pomeroy LR, Wiebe WJ. 2001. Temperature and substrates as interactive limiting factors for marine heterotrophic bacteria. *Aquat Microb Ecol* **23**: 187–204.

Pomeroy LR, Williams PJ, Azam F, Hobbie JE. 2007. The microbial loop. *Oceanogr* **20**(2): 28–33.

Porter KG, Feig YS. 1980. The use of DAPI for identification and enumeration of bacteria and blue-green algae. *Limnol Oceanogr* **25**: 943–948.

Prézelin BB, Hofmann EE, Mengelt C, Klinck JM. 2000. The linkage between Upper Circumpolar Deep Water (UCDW) and phytoplankton assemblages on the west Antarctic Peninsula continental shelf. *J Mar Res* **58**: 165–202. doi: 10.1357/002224000321511133.

Randall-Goodwin E, Meredith MP, Jenkins A, Yager PL, Sherrell RM, et al. 2015. Freshwater distributions and water mass structure in the Amundsen Sea Polynya region, Antarctica. *Elem Sci Anth* **3**: 000065. doi: 10.12952/journal.elementa.000065.

Richert I, Dinasquet J, Logares R, Riemann L, Yager PL, et al. 2015. The influence of light and water mass on bacterial population dynamics in the Amundsen Sea Polynya. *Elem Sci Anth* **3**: 000044. doi: 10.12952/journal.elementa.000044.

Schoemann V, Becquevort S, Stefels J, Rousseau V, Lancelot C. 2005. *Phaeocystis* blooms in the global ocean and their controlling mechanisms: A review. *J Sea Res* **53**: 43–66. doi: 10.1016/j.seares.2004.01.008.

Schofield O, Ducklow HW, Martinson DG, Meredith MP, Moline MA, et al. 2010. How do polar marine ecosystems respond to rapid climate change? *Science* **328**(5985):1520–1523.

Schofield O, Travis M, Alderkamp AC, Lee S, Haskins C, et al. 2015. *In situ* phytoplankton distributions in the Amundsen Sea polynya measured by autonomous gliders. *Elem Sci Anth* **3**: 000073. doi: 10.12952/journal.elementa.000073.

Segel IH. 1975. *Enzyme kinetics*. John Wiley & Sons.

Sherr EB, Sherr BF. 2002. Significance of predation by protists in aquatic microbial food webs. *Antoine van Leeuwenhoek* **81**: 293–308.

Sherrell RM, Lagerström M, Forsch KO, Stammerjohn SE, Yager PL. 2015. Dynamics of dissolved iron and other bioactive trace metals (Mn, Ni, Cu, Zn) in the Amundsen Sea Polynya, Antarctica. *Elem Sci Anth* **3**: 000071. doi: 10.12952/journal.elementa.000071.

Simon M, Azam F. 1989. Protein content and protein synthesis rates of planktonic marine bacteria. *Mar Ecol-Prog Ser* **51**: 201–213.

Simon M, Grossart HP, Schweitzer B, Ploug H. 2002. Microbial ecology of organic aggregates in aquatic ecosystems. *Aquat Microb Ecol* **28**: 175–211

Smith DC, Azam F. 1992. A simple, economical method for measuring bacterial protein synthesis rates in seawater using ^{3}H-leucine. *Mar Microb Food Webs* **6**(2): 107–114.

Smith Jr WO, Ainley DG, Arrigo KR, Dinniman MS. 2014. The oceanography and ecology of the Ross Sea. *Annu Rev Mar Sci* **6**: 469–487. doi: 10.1146/annurev-marine-010213-135114.

Smith Jr WO, Barber DG (eds). 2007. *Polynyas: Windows to the World*. Amsterdam: Elsevier Science. 474 pp. (Elsevier Oceanography Series, Vol. 74).

Smith Jr WO, Shields AR, Dreyer JC, Peloquin JA, Asper V. 2011. Interannual variability in vertical export in the Ross Sea: Magnitude, composition, and environmental correlates. *Deep-Sea Res Pt I* **58**(2): 147–159.

Smith Jr WO, Tozzi S, Long MC, Sedwick PN, Peloquin JA, et al. 2013. Spatial and temporal variations in variable fluorescence in the Ross Sea (Antarctica): Oceanographic correlates and bloom dynamics. *Deep-Sea Res Pt I* **79**: 141–155.

Sokal RR, Rohlf FJ. 1995. *Biometry. The Principles and Practice of Statistics in Biological Research*, 3rd Edition. New York: WH Freeman and Company. 859 pp.

Stammerjohn SE, Maksym T, Massom RA, Lowry KE, Arrigo KR, et al. 2015. Seasonal sea ice changes in the Amundsen Sea, Antarctica, over the period of 1979–2014. *Elem Sci Anth* **3**: 000055. doi: 10.12952/journal.elementa.000055.

Stammerjohn SE, Martinson DG, Smith RC, Iannuzzi RA. 2008. Sea ice in the western Antarctic Peninsula region: Spatio-temporal variability from ecological and climate change perspectives. *Deep-Sea Res Pt II* **55**(18–19): 2041–2058. doi: 10.1016/j.dsr2.2008.04.026.

Steinberg DK, Carlson CA, Bates NR, Goldthwait SA, Madin LP, et al. 2000. Zooplankton vertical migration and the active transport of dissolved organic and inorganic carbon in the Sargasso Sea. *Deep-Sea Res Pt I* **47**: 137–158.

Steinberg DK, Nelson NB, Carlson CA, Prusak AC. 2004. Production of chromophoric dissolved organic matter (CDOM) in the open ocean by zooplankton and the colonial cyanobacterium *Trichodesmium* spp. *Mar Ecol-Prog Ser* **267**: 45–56.

Steinberg DK, Van Mooy BAS, Buesseler KO, Boyd PW, Kobari T, et al. 2008. Bacterial vs. zooplankton control of sinking particle flux in the ocean's twilight zone. *Limnol Oceanogr* **53**(4): 1327–1338.

Suttle CA. 2007. Marine viruses - major players in the global ecosystem. *Nature Reviews: Microbiology* **5**: 801–812. doi: 10.1038/nrmicro1750.

Tagliabue A, Arrigo KR. 2003. Anomalously low zooplankton abundance in the Ross Sea: An alternative explanation. *Limnol Oceanogr* **48**(2): 686–699.

Tang KW, Jakobsen HH, Visser AW. 2001. *Phaeocystis globosa* (Prymnesiophycae) and the planktonic food web: Feeding, growth, and trophic interactions among grazers. *Limnol Oceanogr* **46**(8): 1860–1870.

Tynan CT. 1998. Ecological importance of the southern boundary of the Antarctic Circumpolar Current. *Nature* **392**: 708–710.

Vaqué D, Guixa-Boixereu N, Gasol JM, Pedrós-Alió C. 2002. Distribution of microbial biomass and importance of protists in regulating prokaryotic assemblages in three areas close to the Antarctic Peninsula in spring and summer 1995/96. *Deep-Sea Res Pt II* **49**: 847–867.

Vernet M, Martinson D, Iannuzzi R, Stammerjohn S, Kozlowski W, et al. 2008. Control of Primary Production by Sea Ice Dynamics west of the Antarctic Peninsula. *Deep-Sea Res Pt II* **55**: 2068–2085.

Vetter YA, Deming JW, Jumars PA, Krieger-Brockett BB. 1998. A predictive model of bacterial foraging by means of freely released extracellular enzymes. *Microb Ecol* **36**(1): 75–92.

Wilson SE, Swalethorp R, Kjellerup S, Wolverton MA, Ducklow HW, et al. 2015. Meso- and macro-zooplankton community structure of the Amundsen Sea Polynya, Antarctica (Summer 2010–2011). *Elem Sci Anth* **3**: 000033.

Yager PL, Connelly TL, Mortazavi B, Womack KE, Bano N, et al. 2001. Dynamic bacterial and viral response to an algal bloom at sub-zero temperatures. *Limnol Oceanogr* **46**: 790–801.

Yager PL, Sherrell RM, Stammerjohn SE, Alderkamp AC, Schofield O, et al. 2012. ASPIRE: The Amundsen Sea Polynya International Research Expedition. *Oceanogr* **25**(3): 40–53. doi: 10.5670/oceanog.2012.73.

Yager PL, Sherrell RM, Stammerjohn SE, Ducklow HW, Schofield OME, et al. 2016. A carbon budget for the Amundsen Sea Polynya, Antarctica: Estimating net community production and export in a highly productive polar ecosystem. *Elem Sci Anth*: Under review for the ASPIRE Special Feature.

Contributions

- Contributed to conception and design: PY
- Contributed to acquisition of data: CW, JL, AP, JD, and PY
- Contributed to analysis and interpretation of data: CW, AD, JL, AP, JD, and PY
- Drafted and or revised the article: CW, AP, JD, PY
- Approved the submitted version for publication: CW, AD, JL, AP, JD, PY

Acknowledgments

We thank the following persons and groups for contributions to this manuscript: Raytheon Polar Services (in particular, Lindsey Ekern for nutrient analysis onboard) and the captain and crew of the *R.V. Nathaniel B. Palmer* for providing logistical support at sea; Yager lab group members for help with running samples at sea, data analysis, and general support, especially K. Sines, T. Connelly, B. Page, L. Mu, and M.K. Crews; ASPIRE team members for contributing data: especially A. Alderkamp and G. van Dijken (chlorophyll *a*), L. Riemann (virus counts), R. Logares (flagellates), R. Swalethorp, S. Kjellerup, and T. Nielsen (ciliates), O. Schofield (HPLC and primary production), E. Ingall (dissolved organic matter), R. Sherrell and M. Lagerström (particulate organic carbon and nitrogen), K. Lowry (sea ice cover), S. Wilson (macrozooplankton), and S. Stammerjohn (hydrography); S. Holland and B. Tolar for contributing code and 'R' support for PCA analysis. The authors thank the editor and two anonymous reviewers for their thorough and constructive improvements to the manuscript.

Funding information

This research was supported by a grant awarded to PLY from the National Science Foundation, Office of Polar Programs, Antarctic Organisms and Ecosystems (ANT-0839069). We also acknowledge support for participation of AFP by NSF (ANT-0839012 to Hugh Ducklow) and for Swedish collaborators from the Swedish Research Council (#2008-6430 to S. Bertilsson and L. Riemann). Partial support also came from a graduate teaching assistantship awarded to CMW from UGA Marine Sciences.

Competing interests

Authors have no competing interests or conflicts of interest.

Data accessibility statement

All data used in this paper will be submitted to BCO-DMO before publication.